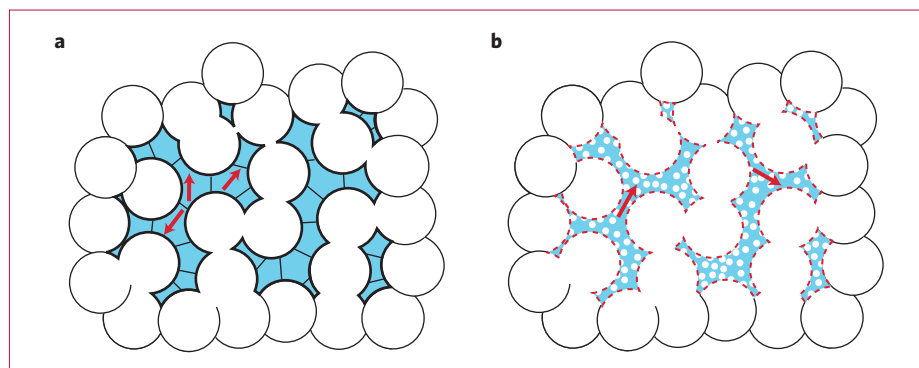In the present article[3], the authors report on their efforts to increase the strain by opening pores in the struts themselves to eliminate the nodes. Once the nodes are eliminated, the single crystallinity of such foams can extend over longer distances. The authors do indeed largely succeed by selecting space holders that give rise to a bimodal size distribution in the foam with extra smaller pores having dimensions smaller than the struts themselves (Fig. 2b). Under optimized conditions, field-induced strains in the order of 4–5% are attained.

The preparation of foams with such large field-induced strains can be considered a breakthrough in magnetic shape-memory technology. Limitations certainly remain, especially those related to attaching a load that causes a reduction in strain in single crystals. This will definitely be an issue that has to be dealt with in foams as well. Nevertheless, many ideas for the use of the magnetic shape-memory materials in diverse technological applications, such as micropumps, sonars and magnetomechanical sensors, to name but a few — and originally considered suitable only for single crystals — can now be largely realized with the use of foams.

Over many years, worldwide research on magnetic shape memory has not been limited to Ni–Mg–Ga, and much work has been carried out in the past decade on alternative systems[6]. These investigations have given rise to the observation of many other effects apart from field-induced strains, such as the magnetocaloric effect, giant magnetoresistance, exchange bias, and so on. Certainly, the present work on Ni–Mg–Ga foams with bimodal pore-size distribution will create new avenues of research on other potential magnetic shape-memory alloy foams in general, yielding many fresh and interesting results. ❑

Figure 2 | Magnetic shape-memory foams. **a**, Foam with monomodal pore distribution. The foam material is the blue area bounded by the bold line. Red arrows indicate the easy-magnetization axes. Struts are bounded by polycrystalline nodes (lines traversing the material) limiting field-induced strain. **b**, Foam with bimodal foam distribution. The material is within the same blue area (outlined by the red dashed lines) as in **a**. Nodes are eliminated and the crystal grain can extend over longer distances, yielding a large field-induced strain.

Mehmet Acet is in the Physics Department, University of Duisburg-Essen, D-47048, Duisburg, Germany.
e-mail: mehmet.acet@uni-due.de

References
1. Ullakko, K. *et al. Appl. Phys. Lett.* **69,** 1966–1968 (1996).
2. Sozinov, A. *et al. Appl. Phys. Lett.* **80,** 1746–1749 (2002).
3. Chmielus, M., Zhng, X. X., Witherspoon, C., Dunand, D. C. & Mullner, P. *Nature Mater.* **8,** 863–866 (2009).
4. Tellinen, J. *et al.* in *Proc. 8th Int. Conf. on New Actuators, Actuator 2002* (ed. Borgmann, H.) 566–569 (Messe Bremen, 2002).
5. Boonyyongmaneerat, Y. *et al. Phys. Rev. Lett.* **99,** 247201 (2007).
6. Planes A., Mañosa, L. & Acet, M. *J. Phys. Condens. Matter* **21,** 233201 (2009).

BIODEGRADABLE ALLOYS

The glass window of opportunities

Crystalline alloys often fall short in providing certain key properties desired for biomedical applications. But by using metallic glasses instead, problems such as hydrogen evolution can be dramatically reduced in biodegradable magnesium alloys.

Evan Ma and Jian Xu

Crystalline metallic alloys constitute an important group of biomedical materials, thanks to their unique combination of strength, ductility, fatigue resistance and reliability. Magnesium alloys, in particular, are being increasingly investigated for biomedical applications such as implants and stents[1–6]. This pursuit of Mg alloys is motivated by their low mass density (ρ = 1.74–2.0 g cm^{-3}) and elastic modulus (Young's modulus E of 41–45 GPa), both of which are similar to those of human bones (ρ = 1.8–2.1 g cm^{-3}; E = 3–20 GPa). Importantly, Mg alloys

have high biocompatibility, and are biodegradable and also relatively inexpensive. However, despite these attractive properties, existing Mg alloys do suffer from serious drawbacks, one of which is that Mg corrodes too quickly in physiological conditions, into soluble magnesium hydroxide, magnesium chloride and hydrogen gas[4]. In particular, hydrogen evolution leads to gas pockets that cause adverse reactions and inhibit bone growth. On page 887 of this issue[7], Zberg *et al.* circumvent this problem by using ternary Mg–Zn–Ca alloys in the form of metallic

glasses[8]. In their *in vitro* and *in vivo* degradation tests, these amorphous alloys show tissue compatibility as good as that of their crystalline counterparts, but without clinically observable hydrogen production.

In the past, all the alloys used for orthopaedics and coronary stents were adapted from existing alloys used in engineering, which are, of course, all crystalline materials. Examples include stainless steels, Co–Cr–Mo alloys, Ti alloys, and Ti–Ni shape-memory alloys. However, as these conventional alloys have not been specifically designed for particular

biomedical needs, problems inevitably arise in long-term clinical applications, such as excessive mismatch in stiffness with the bone, release of toxic elements and incompatibility with X-ray or magnetic resonance imaging. Therefore, the systematic attempt by Zberg et al.[7] to pursue a completely new family of metallic alloys specifically for bioimplant applications is refreshing and potentially very rewarding.

Metallic glasses are prepared by fast-cooling molten alloys to below their glass-transition temperature, which avoids crystallization altogether[8]. Often this is achieved in a copper mould, which aids the rapid extraction of heat to allow the high cooling rate to be reached. These glasses retain the amorphous structure of the parent liquid alloy. As such, metallic glasses are chemically homogeneous alloys, with the contents of alloying elements (such as Zn in Mg) extending to well beyond the solubility that could be achieved at equilibrium when the molten alloy is cooled slowly. As shown in Fig. 1, there is a fairly

wide composition range over which the three biocompatible elements — Mg, Zn and Ca — can be intimately mixed on the atomic level into a single-phase Mg–Zn–Ca glass. In the glass-forming composition range shown in Fig. 1 (Zn content from 21 to 35 at.%), metallic glass rods that have a critical diameter (D_c) of at least 1 mm can be fabricated — this size corresponds to a cooling rate of 10^2–10^3 K s^{-1}. This window allows the tuning of the Zn concentration to levels sufficiently high to partially passivate the surface. Specifically, with over ~28 at.% Zn in the alloy, the corrosion mechanism in a physiological environment changes, and a dense amorphous layer rich in Zn and oxygen is formed, which protects the surface and reduces hydrogen production to acceptable levels[7].

This alteration of corrosion behaviour is impossible in crystalline alloys, because at such Zn concentrations they would evolve into crystallites of several intermetallic compounds with very different Zn contents, fixed by equilibrium solubility limits. These equilibrium phases would remove

the opportunity to continuously adjust the Zn concentration and hence to control the product and the degradation rate. They would also produce interphase and grain boundaries that could be the weak spots for corrosion to begin. In this respect, the glasses have a clear edge over their crystalline counterparts.

The unprecedented opportunities that metallic glasses bring to the table are not limited to corrosion performance. Owing to the absence of crystalline lattice and the associated dislocation defects in the internal structure, the metallic glasses have strengths several times higher than those of the crystalline Mg alloys. This is in fact a significant benefit, as the relatively low strength of common commercial Mg alloys is the other principal roadblock limiting their applications in biomedical devices. And as well as being wear resistant, metallic glasses — like plastics — can be moulded in the supercooled-liquid regime (that is, at temperatures above the glass-transition temperature but below the crystallization temperature) for net-shaping of complex geometries. Net-shaping is moulding directly into the desired shape without the need for subsequent machining (such as blowing a glass).

When dealing with glasses, low ductility could be a concern for applications within the body where they will be placed under stresses, and shattering would be disastrous. However, in contrast to our classic idea of window glasses, metallic glasses do have deformation mechanisms that allow them to yield and plastically flow when the stresses are very high[8–12]. For metallic glasses with micrometre or submicrometre dimensions, significant deformability without catastrophic failure[9–11], including tensile ductility and necking[11], has been previously demonstrated. In fact, in another recent publication, Zberg et al.[12] reported tensile ductility of their Mg–Zn–Ca glass wires at a stress level as high as ~800 MPa.

Considering the suite of properties and advantages discussed above, metallic glasses do seem to have great potential that is worth exploring, at least for certain niche applications[13], such as small biodegradable devices. However, the Mg–Zn–Ca glass is a metastable phase with a relatively low glass-transition temperature[14,15]; its structural stability in long-term service, and the associated chemical and mechanical behaviour — such as potential embrittlement[16] — will require further examination.

On the one hand, metallic glasses hold much promise for improving next-generation biodegradable implants. On the other hand, the newly discovered
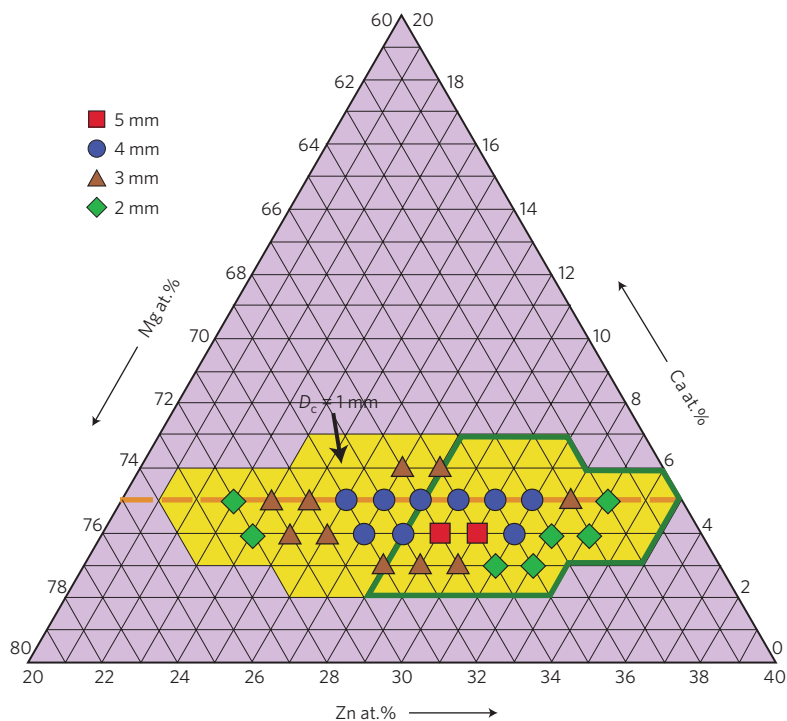
Figure 1 | The composition range (yellow area) over which Mg–Zn–Ca alloys can be produced in the form of bulk metallic glasses by means of copper-mould casting (Y. Y. Zhao and J. Xu, unpublished results). A bulk metallic glass is defined as a fully amorphous metallic glass when its critical size D_c (diameter or the size of the thinnest dimension) exceeds 1 mm. At certain compositions, a D_c larger than 1 mm can be achieved (see the various symbols in the legends). Note that the smaller the D_c, the larger the composition range for glass formation: for the 50–500-μm-thick glass foils fabricated by Zberg et al.[7], the glass-forming composition range will be larger than the yellow area. The compositions of the metallic-glass series studied in ref. 7, $Mg_{60+x}Zn_{35-x}Ca_5$ ($0 < x < 15$), are marked with an orange line. The region that satisfies the >28 at.% Zn requirement for greatly reduced hydrogen generation during biodegradation[7] is encircled by a solid green line.

application, in return, opens virgin territory that raises the future worth of metallic glasses themselves. Indeed, broadening the scope of critical applications for metallic glasses is a key challenge facing the metallic-glass research community today. This interdisciplinary advance[7] is thus a timely and welcome stimulus for both fields. ❑

Evan Ma is in the Department of Materials Science and Engineering, The Johns Hopkins University, Baltimore, Maryland 21218, USA; Jian Xu is at the Shenyang National Laboratory for Materials Science, Institute of Metal Research, Chinese Academy of Sciences, Shenyang, 110016, China.
e-mail: ema@jhu.edu; jianxu@imr.ac.cn

References
1. Staiger, M. P., Pietak, A. M., Huadmai, J. & Dias, G. Biomaterials 27, 1728–1734 (2006).
2. Witte, F. et al. Biomaterials 26, 3557–3563 (2005).
3. Erbel, R. et al. Lancet 369, 1869–1875 (2007).
4. Mani, G., Feldman, M. D., Patel, D. & Agrawal, C. M. Biomaterials 28, 1689–1710 (2007).
5. Zeng, R., Dietzel, W., Witte, F., Hort, N. & Blawert, C. Eng. Mater. 10, B3–B14 (2008).
6. Von Der Höh, N. et al. Adv. Eng. Mater. 11, B47–B54 (2009).
7. Zberg, B., Uggowitzer, P. J. & Löffler, J. F. Nature Mater. 8, 887–891 (2009).
8. Greer, A. L. & Ma, E. MRS Bull. 32, 611–615 (2007).
9. Shan, Z. W. et al. Phys. Rev. B 77, 155419 (2008).
10. Volkert, C. A., Donohue, A. & Spaepen, F. J. Appl. Phys. 103, 083539 (2008).
11. Guo, H. et al. Nature Mater. 6, 735–739 (2007).
12. Zberg, B., Arata, E. R., Uggowitzer, P. J. & Löffler, J. F. Acta Mater. 57, 3223–3231 (2009).
13. Schroers, J., Kumar, G., Hodges, T., Chan, S. & Kyriakides, T. J. Min. Mater. Met. S. 61, 21–29 (2009).
14. Gu, X., Shiflet, G. J., Guo, F. Q. & Poon, S. J. J. Mater. Res. 20, 1935–1938 (2005).
15. Zhao, Y. Y., Ma, E. & Xu, J. Scripta Mater. 58, 496–499 (2008).
16. Castellero, A., Uhlenhaut, D. I., Moser, B. & Löffler, J. F. Phil. Mag. Lett. 87, 383–392 (2007).

CARBON NANOTUBES

Not that slippery

Friction measurements on carbon nanotubes show a remarkable anisotropy, the origin of which can be traced to the activation of specific deformation modes of energy dissipation.

Ruben Perez

Sliding friction is one of the oldest problems in physics and materials science. Almost every aspect of everyday life involves the contact of two solid surfaces, and the effort to minimize the energy lost during their relative displacement has occupied some of the brightest minds in history, including Leonardo da Vinci. Understanding the fundamental origin of friction has become an even more pressing challenge with the miniaturization of moving components in many commercial products, including computer-disk heads and the microelectromechanical systems that trigger the airbags in our cars. Carbon nanotubes (CNTs) are one of the most promising building blocks to scale these devices down to the nanometre scale. On page 876 of this issue, Lucas et al.[1] explore the tribological properties of CNTs, and show that friction forces are different when sliding a nanosized tip parallel or perpendicular to the CNT axis. With the aid of molecular-dynamics simulations, they are able to identify the microscopic dissipation mechanism responsible for this anisotropic behaviour and its connection with some fundamental properties of the nanotubes, such as their chirality.

The old, simple empirical laws that govern friction at the macroscopic scale are the result of the collective behaviour of the many different asperities that define the real contact area between two rough surfaces. Modern nanotribology aims to explore the 'single asperity' level relevant
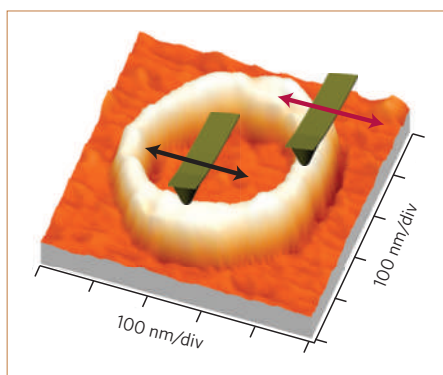
Figure 1 | Schematic of the experiment, showing the AFM topography of a 7 nm nanotube and the scanning direction of the AFM tip parallel (black arrow) or perpendicular (red arrow) to the nanotube axis.

for nanometre-scale junctions[2,3]. The atomic force microscope (AFM) is the tool of choice for measuring the normal and lateral forces during the sliding of the nanometre-radius tip of the AFM on a given surface. Lucas et al. follow this approach to determine the friction properties of multiwall CNTs deposited on a silicon substrate (Fig. 1). Their measurements confirm that the simple linear relationship (that we learn at school) between the friction force and the applied load is replaced by a two-thirds power-law dependence at these nanometre-scale contacts. More surprisingly, they found that, for nanotubes with radii

smaller than 10 nm, friction forces are different when the tip slides parallel or perpendicular to the CNT axis. The shear strength, which is the proportionality factor between the friction force and the contact area, can be as much as three times larger for the transverse sliding for a CNT with a radius of 4 nm.

In the absence of wear (that is, no permanent damage of the tip and/or sample), friction arises from the transfer of collective translational kinetic energy into nearly random heat motion. Understanding the fundamental microscopic mechanisms involved in this process is one of the great challenges in nanotribology. Mechanical energy can be directly converted into vibrations of the surface and tip atoms in the contact. These vibrations are expected to be damped by energy transfer to bulk phonon modes, and by electronic excitations of charge carriers (for example, the creation of electron–hole pairs in metals, the creation of electronic surface states that are charged and then discharged on release of the stress, and tip-induced hopping of trapped charges).

Recent experiments that focus on the control of one of these possible mechanisms have shown the dependence of friction force on carrier concentration in silicon p–n junctions[4], and the effect of changes in the mass of the surface atoms (and thus, in their vibrational properties)[5]. Differences in friction between single and bilayer graphene films have been related to a dramatic difference in electron–phonon